

# Synthesis and reactivity of a $C_3$ -symmetric trinuclear zinc(II) hydroxide catalyst efficient at phosphate diester transesterification†‡

Ranjan Mitra, Matthew W. Peters and Michael J. Scott\*

Received 27th April 2007, Accepted 14th June 2007

First published as an Advance Article on the web 18th July 2007

DOI: 10.1039/b706386e

Inspired by trinuclear Zn(II) sites in enzymatic systems, a ligand system containing three preorganized (2-pyridyl)methyl piperazine moieties anchored onto a rigid  $C_3$ -symmetric triphenoxymethane platform has been developed for preorganizing three zinc ions into an environment conducive to intramolecular interaction. Zinc(II) binding by this ligand has been analyzed by means of potentiometric measurements in 50% (v/v)  $\text{CH}_3\text{CN}-\text{H}_2\text{O}$  solutions. Subsequently a  $C_3$ -symmetric trinuclear Zn(II) hydroxide complex of the  $C_3$ -symmetric ligand was synthesized and fully characterized using NMR spectroscopy and X-ray crystallography. This complex induces a 16 900-fold rate enhancement in the catalytic cyclization of the RNA model substrate, 2-hydroxypropyl-*p*-nitrophenyl phosphate (HPNP, pH 6.7, 25 °C) over the uncatalyzed reaction with multiple catalyst turnovers. The observed differences in the pH-rate profile can be attributed to the varying concentration of various trinuclear zinc species. The trinuclear Zn(II) catalyst exhibits a higher hydrolytic activity compared to its mononuclear analogue. The reactivity and structural features of this trinuclear Zn(II) complex will be discussed.

The phosphodiester that form the structural backbone of nucleic acids are extremely resistant to hydrolytic cleavage. The estimated half-life of RNA is 110 years and that of DNA is in the range of 10–100 billion years.<sup>1,2</sup> As a consequence, nature has to use various enzymes to accelerate the hydrolysis and to enable the processing of nucleic acids under physiological conditions. Most phosphodiesterases contain two or even three divalent metal ions close to each other, which work synergistically as a single unit.<sup>3–6</sup> The well studied dinuclear zinc phosphatase includes phosphotriesterase<sup>7,8</sup> and alkaline phosphatase.<sup>9,10</sup> Enzymes that incorporate three zinc centers are also known such as phospholipase  $C^{11–13}$  and nuclease P1.<sup>14,15</sup> In these systems, there are two closely associated Zn(II) centers together with a more distant Zn(II) ion. For example, while the separation of the principal dizinc unit in phospholipase C is 3.3 Å, the distances between these centers and the third zinc center are 4.7 and 6.0 Å.<sup>3</sup> Likewise the corresponding separations in P1 nuclease are 3.2, 4.7 and 5.8 Å.<sup>3,14</sup> It is postulated that in P1 nuclease, the hydroxide bridging the two closely associated Zn(II) centers attacks the phosphate substrate that is bound to the third, more distant, Zn(II) ion in a bidentate mode.<sup>14,15</sup> Despite extensive investigations, however, details of the mechanism of this and other metallohydrolases remain controversial. One crucial aspect under debate is the identity and the exact binding mode of the nucleophile.<sup>16,17</sup> Also, the function of a third metal ion in close proximity of a dinuclear metal cluster in these enzymes is not yet fully understood. A diverse assortment of ligands have been employed to model various aspects of multinuclear zinc

enzymes.<sup>2,18–25</sup> By using a variety of spacers, two or more simple ligands, each capable of binding one zinc ion, can be linked together by groups ranging from simple aliphatic chains to more complex groups such as calix[*n*]arenes.<sup>26–41</sup> Other approaches have focused on the large macrocycles that encompass two or more metal ions into a single framework,<sup>42–52</sup> oftentimes producing very effective structural models for these metallohydrolases.<sup>53</sup>

Synthetic analogues that mimic all aspects of these zinc enzymes *i.e.* structure, function, and mechanism, are yet to be obtained. Many of the structural models are inactive for catalysis,<sup>20</sup> while in functional models it is frequently difficult to discern the identity of the competent catalysts since the molecules are often prepared *in situ*.<sup>20</sup> Thus, to have a better understanding of the catalytic mechanism, it could be advantageous to combine both structural and functional information into a single system. With these issues in mind, a simple ligand capable of preorganizing three metal ions into an environment conducive to intramolecular interaction was designed using the  $C_3$ -symmetric triphenoxymethane as a platform.<sup>54</sup> In this paper we describe the synthesis of ligand **5** using the  $C_3$ -symmetric triphenoxymethane platform, the formation of the corresponding Zn(II) complex and its catalytic activity in the cleavage of the phosphate diester bond of an RNA model substrate.

## Results and discussion

### Ligand synthesis and structural characterization of **5** and **7**

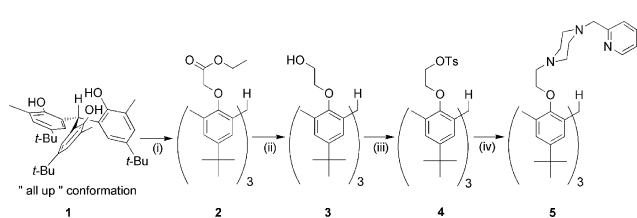
To develop a synthetic model for the trinuclear zinc enzymes, three nitrogen based ligands, each capable of binding one zinc ion, can be attached to a platform capable of reorganizing these moieties into an environment conducive to intramolecular interactions between the three bound metal ions. Previous work with a triphenoxymethane platform has shown that, when all the three phenol oxygens are substituted, the conformation with these oxygen atoms “all up” relative to the central methine hydrogen of the platform

Department of Chemistry and Center for Catalysis, University of Florida, Gainesville, FL, 32611-7200, USA. E-mail: mjscott@chem.ufl.edu; Fax: +1 352 392-3255; Tel: +1 352 846-1165

† CCDC reference numbers 645249 and 645250. For crystallographic data in CIF or other electronic format see DOI: 10.1039/b706386e

‡ Electronic supplementary information (ESI) available: Synthetic procedures and characterization data for **8**, **9**, **10**, **11**. <sup>1</sup>H NMR spectra of **7** in the presence of buffer at pH = 6.7. See DOI: 10.1039/b706386e

exclusively exists both in the solid state and in solution.<sup>54</sup> Extended arms can easily be secured to the phenolic oxygens (Scheme 1). NMR spectral data and the X-ray crystal structure of **5** (Fig. 1) illustrate that indeed, the conformation of the platform is “all up” and that the three metal binding sites are preorganized and poised for modeling biological trinuclear active sites.



**Scheme 1** Synthesis of ligand **5**. Reagents and conditions: (i) 3.3 equiv.  $\text{BrCH}_2\text{COOEt}$ , 4 equiv.  $\text{Cs}_2\text{CO}_3$ , acetone, reflux (ii) 6 equiv.  $\text{LiAlH}_4$ ,  $\text{Et}_2\text{O}$  (iii) 4 equiv.  $p\text{-CH}_3\text{C}_6\text{H}_4\text{SO}_2\text{Cl}$ , pyridine (iv) 30 equiv. 1-[(2-pyridyl)methyl]piperazine, 10 equiv.  $\text{Na}_2\text{CO}_3$ , acetonitrile, 5 d reflux.

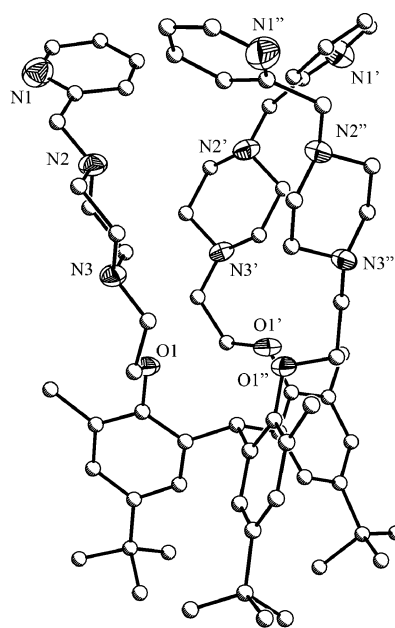


**Fig. 1** The X-ray crystal structure of **5** drawn with 30% ellipsoids (carbons with arbitrary radii). Hydrogen atoms omitted for clarity.

Addition of three equivalents of  $\text{Zn}(\text{ClO}_4)_2 \cdot 6\text{H}_2\text{O}$  to a solution of **5**, afforded the trinuclear zinc(II) complex, **7**. The solid-state structure of **7**, as determined by X-ray crystallography, is shown in Fig. 2 and selected bond lengths and angles are given in Table 1. In the solid state, the molecule possesses rigorous  $C_3$ -symmetry with a distance of 3.43 Å between the zinc centers. The three zinc cations are assembled into a distorted six-membered ring connected together by three bridging hydroxyl groups, and the angle about the zinc and hydroxides differ significantly [ $\text{O1-Zn1-O1}'$  109.4(2)° and  $\text{Zn1-O1-Zn1}'$  127.6(2)°]. The metal hydroxide distances are typical for a  $\text{Zn}_3(\text{OH})_3$  core and differ slightly [1.925(4) Å,  $\text{Zn1-O1}$ ; 1.903(4) Å,  $\text{Zn1-O1}'$ ].<sup>55–57</sup> The zinc nitrogen separations are asymmetric with a bond length of 2.055(5) Å to the pyridyl nitrogen and 2.143(5) Å to the piperazine nitrogen. The metal maintains a highly distorted tetrahedral geometry with bond angles ranging from 81.0(2)° [ $\text{N1-Zn1-N2}$ ] to 127.28(19)°

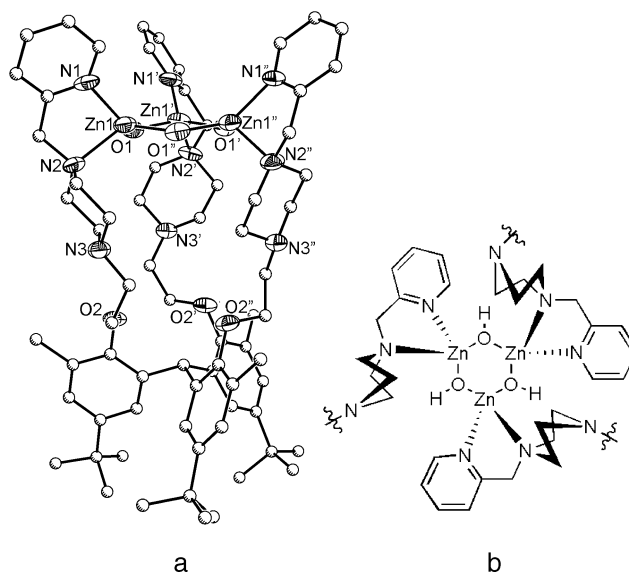


**Fig. 2** Depiction of the solid-state structure of **7** (a) Side view with hydrogen atoms and perchlorate anions omitted for clarity (30% probability ellipsoids, carbon atoms arbitrary radii). Primed and unprimed atoms are related by a 3-fold symmetry axis. (b) Cartoon of the top view of the core.

**Table 1** Selected interatomic distances and angles for **7**·3(Me)<sub>2</sub>CO

Bond lengths/Å		Bond angles/°	
Zn1–O1	1.925(4)	N1–Zn1–N2	81.0(2)
Zn1–O1''	1.903(4)	N1–Zn1–O1	111.7(2)
Zn1–N1	2.055(5)	N1–Zn1–O1''	127.28(19)
Zn1–N2	2.143(5)	N2–Zn1–O1''	104.3(2)
Zn...Zn	3.435	O1–Zn1–O1''	109.4(2)
		N2–Zn1–O1	121.01(19)

[ $\text{N2-Zn1-O1}$ ]. Three perchlorate anions balance the charge on the complex. Similar coordination geometries have been observed in a few *N*-methylpiperazine and morpholine based ligands.<sup>58</sup> Although, the  $\text{Zn}_3(\text{OH})_3$  structural core has been obtained previously from self-assembly reactions with small ligands, to the best of our knowledge, hydrolytic cleavage of phosphate diester bonds using these complexes has not yet been reported.<sup>55–57</sup>

The NMR spectrum of the ligand undergoes significant changes upon incorporation of zinc ions into the ligand (see ESI†, Fig. S1, S2). The resonance for the central methine proton shifts downfield from 6.52 ppm in **5** to 7.10 ppm in **7**. The coordination of zinc by the ligand arms forms new cyclic structures that result in the splitting and shifting of various peaks, especially those associated with the (2-pyridyl)methyl piperazine moiety. Fluctuations in the linker moieties connecting these groups to the triphenoxymethane platform and within the coordination sphere of the metal cause these split peaks to appear broadened in the spectra. <sup>1</sup>H NMR spectroscopy suggests that on the NMR time scale a  $C_3$ -symmetric core is maintained in solution, under the conditions (pH 6.7, 50% (v/v)  $\text{CD}_3\text{CN-D}_2\text{O}$ , buffer,  $[\mathbf{7}] = 7.5 \text{ mM}$ ) used for the kinetic experiments described below. The species distribution diagram depicted in Fig. 6, (*vide infra*), however, indicated the presence of various trinuclear zinc species in solution at and around pH 6.7, suggesting a proton exchange reaction occurs quite fast in these solutions.<sup>59</sup> All solutions remained clear during the time of the

kinetic experiments and no peak corresponding to the free ligand was observed. After prolonged periods at pH 6.7, however, peaks corresponding to the free ligand do appear in the  $^1\text{H}$  NMR spectrum indicating that the metals can be slowly leached out of the ligand. After about 24 h in the absence of HPNP, the system reached chemical equilibrium with the buffer solution containing complex **7** and free ligand **5** in a  $\sim 6:1$  ratio, but under the catalytic condition, within the first 5% conversion of the reactant, the core of **7** is stable with very little free  $\text{Zn(II)}$  or free ligand in solution (see ESI $^\ddagger$ , Fig. S3–S6). Thus the method of initial rates ( $< 5\%$  conversion) was used to study these reactions (*vide infra*).

Fig. 3 shows the variation of the ratio of free ligand (**5**) to trinuclear zinc complex (**7**) as a function of pH after 30 min of mixing. The change in the ligand concentration was followed by measuring the peak area at 8.44 ppm corresponding to a pyridyl proton of the free ligand. The peak area was normalized relative to the peak area of the same proton, at 8.62 ppm, in the trinuclear zinc complex **7**. A gradual decrease in the ratio of free ligand (**5**) to trinuclear zinc complex (**7**) was observed as the pH was raised from pH 5.87 to pH 6.7. Further increasing the pH to 7.01 produced a slight increase in the ratio. Under these conditions, the depletion of Zn may be due to the formation of  $\text{Zn(II)}$ -MES (MES = 2-morpholinoethanesulfonic acid) buffer complex.<sup>60</sup> In the absence of a buffer the 50% (v/v)  $\text{CD}_3\text{CN}-\text{D}_2\text{O}$  solution of **7** is stable for weeks (see ESI $^\ddagger$ , Fig. S4). At higher pH values, the  $\text{Zn(II)}$  complex is increasingly unstable owing to the formation of insoluble zinc hydroxide.

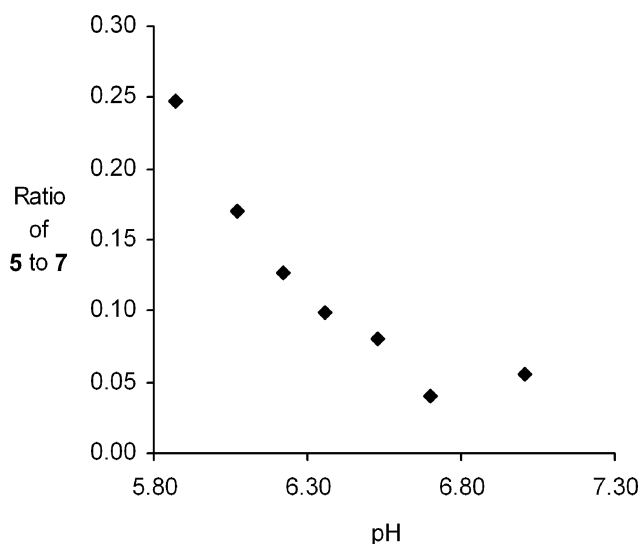


Fig. 3 Variation of the ratio of free ligand (**5**) to trinuclear zinc complex (**7**) as a function of pH.

Fig. 4 shows the temperature dependence of the  $^1\text{H}$  NMR spectrum of the aromatic region of **7** in 50% (v/v)  $\text{CD}_3\text{CN}-\text{D}_2\text{O}$  at pH 6.7 (peaks corresponding to the aliphatic region are not shown as they are masked by the presence of a large excess of MES buffer). Increasing the temperature from 10 °C to 55 °C induced only a minor sharpening of the peaks suggesting that on the NMR time scale the proton exchange between various species in solution is quite fast in this temperature range. The compound precipitates out of solution below 10 °C thus restricting the experiment within a span of 45 °C.

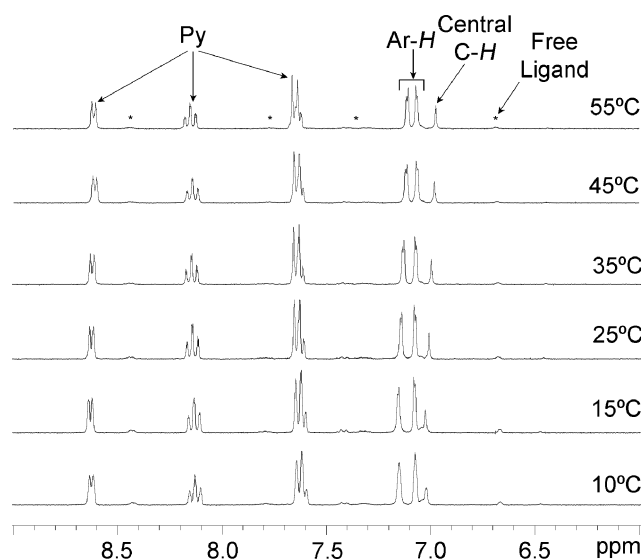


Fig. 4 Temperature-dependent  $^1\text{H}$  NMR spectra of the aromatic region of **7**. The reaction mixture contains **7** (7.5 mM), MES buffer (22.5 mM) in 1 : 1 ( $\text{CD}_3\text{CN}-\text{D}_2\text{O}$ ) at pH = 6.7.

## Solution equilibria

While the X-ray crystallographic results provide structural insights for the various complexes, knowledge of the species distribution in solutions is crucial for understanding any trends in hydrolytic reactivity of artificial metallohydrolases. To investigate the relationship between the pH dependence of these reactions and the structures of the aquo-trizinc complexes in solution, the  $\text{p}K_a$  values of the ligand, **5**, (Table 2), as well as the stability constants of its zinc complexes and the  $\text{p}K_a$  values of zinc bound water molecules in these complexes (Table 3), were determined by pH titrations. Buffer was included in the solutions for all of the NMR experiments but it was omitted from the potentiometric titrations due to the nature of the experiment.

Table 2 Protonation constants of the ligand **5** at 25 °C;  $I = 0.1$  M KCl

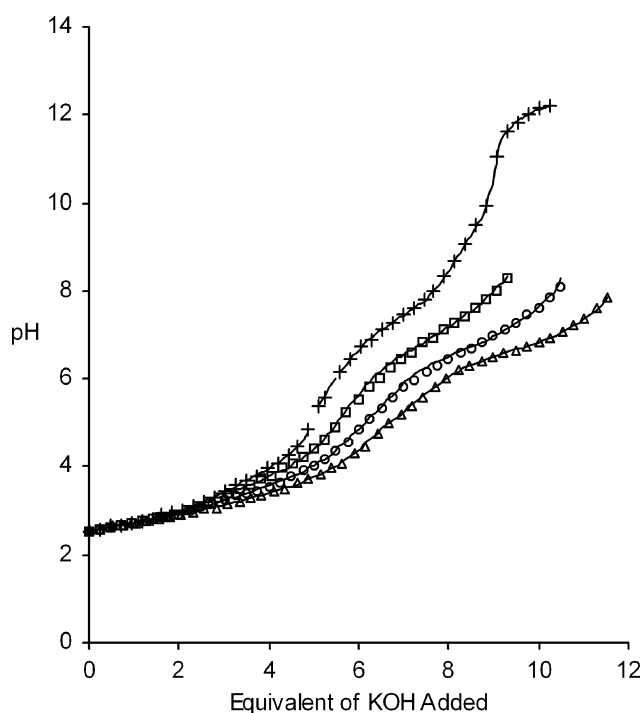
Species	Log $\beta$	$\text{p}K_a$
$[\text{LH}_6]^{6+}$	37.96	3.81
$[\text{LH}_5]^{5+}$	34.15	3.95
$[\text{LH}_4]^{4+}$	30.20	6.10
$[\text{LH}_3]^{3+}$	24.10	7.27
$[\text{LH}_2]^{2+}$	16.83	7.60
$[\text{LH}]^+$	9.23	9.23

Table 3 Stability constants of the  $\text{Zn(II)}$  complexes with **5** at 25 °C;  $I = 0.1$  M KCl

Species	Log $\beta$	$\text{p}K_a$
$[\text{Zn}_3\text{LH}_3]^{9+}$	36.09	4.63
$[\text{Zn}_3\text{LH}_2]^{8+}$	31.46	5.53
$[\text{Zn}_3\text{LH}]^{7+}$	25.93	6.66
$[\text{Zn}_3\text{L}]^{6+}$	19.27	6.50
$[\text{Zn}_3\text{L}(\text{OH})]^{5+}$	12.77	6.89
$[\text{Zn}_3\text{L}(\text{OH})_2]^{4+}$	5.88	7.63
$[\text{Zn}_3\text{L}(\text{OH})_3]^{3+}$	-1.75	

### Ligand protonation constants.

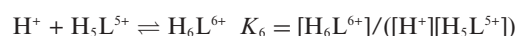
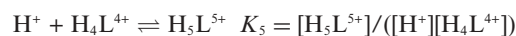
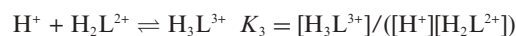
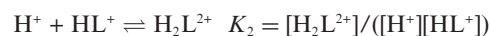
The protonation constant of the ligand was determined by potentiometric titration of **6** (1 mM) with 0.1 M KOH,  $I = 0.1$  M (KCl) at 25 °C. Studies were carried out in 50% (v/v) CH<sub>3</sub>CN–H<sub>2</sub>O mixtures due to the low water solubility of the ligand and the metal complex in pure water. The pH titration curve is shown in Fig. 5. Although the ligand has as many as nine protonation sites (three per side arm), only six measurable deprotonation processes were found in the pH range 2.5 to 11.5. The nitrogen atoms on the pyridyl groups are less basic than those of the aliphatic amines because the former has more s character than the latter.<sup>61</sup> It has also been observed that as the separation between the protonation sites becomes smaller or as the charge on the ligand increases, the successive protonation of the less basic nitrogens becomes progressively more difficult till it reaches a level where protonation is barely accessible in dilute aqueous solutions of low ionic strength.<sup>62</sup>



**Fig. 5** Potentiometric titration curve of **6** with 0 (+), 1 (□), 2 (○) or 3 (Δ) equiv. Zn(II) in 0.1 M KCl in 1 : 1 CH<sub>3</sub>CN–H<sub>2</sub>O at 25 °C.

If only three protons attached to the pyridyl groups are released upon dissolving in a 50% (v/v) CH<sub>3</sub>CN–H<sub>2</sub>O solution of low ionic strength (0.1 M), the initial hydrogen ion concentration will be three times that of the ligand concentration and hence the theoretical initial pH of the solution can be computed as follows:<sup>63</sup>  $\text{pH} = -\log [(3 \times \text{mmol of ligand}) / \text{total volume (mL)}] = -\log [(3 \times 0.046) / 50] = 2.56$ . This value is, in fact, very close to the observed value of 2.53. The first three  $\text{p}K_{\text{a}}$  values are thus below 2.5, and were not considered in the equilibrium model for data analysis. In the following three steps, one proton is removed from each arm, and corresponds to the proton attached to the nitrogen of the piperazinium ion closer to the pyridyl group. The final three deprotonations again correspond to the dissociation of one proton per sidearm, but the protons involved are attached to the other

nitrogen of the piperazinium ion. The titration data were analyzed for the following equilibria. The protonation constants  $K_1$ – $K_6$  are defined as follows:

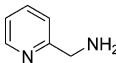
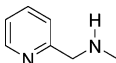
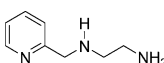
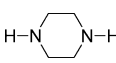
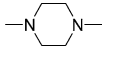


The values of the protonation constants obtained are in agreement with the values of various similar amines in the literature (Table 4).<sup>64</sup> While comparing the values, however, it should be kept in mind that hydrogen bonding with pyridine nitrogen and various other interactions, such as substituent effects where by tertiary amines gain electron density by aliphatic substituents and suffer from a withdrawal of electron density by the picolyl group, have a profound effect on the protonation constant of the ligand.

### Metal complexation in aqueous solution

Titration of the protonated ligand in the presence of 1, 2 and 3 equivalents of Zn(II) were analyzed in batch calculations in which all titration curves were simultaneously fitted with one model (Fig. 6). The accessible pH range has been limited in some of these experiments due to the formation of precipitates. Titrations were stopped as soon as a steady drift was noted in the mV meter reading, indicative of the initiation of the precipitation process. Formation of an insoluble species was observed for pH values higher than pH 8.2, 8.0 and 7.8 for 1 : 1, 1 : 2, and 1 : 3 (L–M) ratios, respectively.

**Table 4**  $\text{p}K_{\text{a}}$  values of similar amines in aqueous solution at 25 °C;  $I = 0.1$  M KCl

Amine	Log $K^{\text{a}}$		
	HL/H <sup>+</sup> L	H <sub>2</sub> L/HL <sup>+</sup> H	H <sub>3</sub> L/H <sub>2</sub> L <sup>+</sup> H
	8.61	2.00	—
	8.91	—	—
	9.46	5.91	2.73
	9.71	5.59	—
	8.13	4.18	—

<sup>a</sup> Values taken from reference <sup>64</sup>.

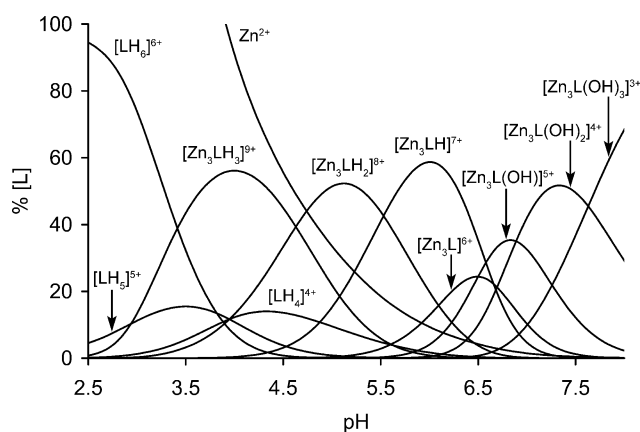
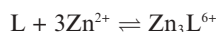
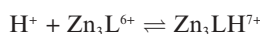


**Fig. 6** Species distribution diagram for **6** (0.92 mM) in the presence of Zn(II) ions (2.76 mM) as a function of pH in 1 : 1 CH<sub>3</sub>CN–H<sub>2</sub>O at 25 °C with *I* = 0.10.

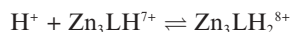
Accordingly, the calculations were carried out using data obtained below their respective pH values. Best fit of the titration data could be attained using the following equilibrium model



$$K_{Zn_3L} = [Zn_3L^{6+}] / [L][Zn^{2+}]^3$$



$$K_{Zn_3LH} = [Zn_3LH^{7+}] / [H^+][Zn_3L^{6+}]$$



$$K_{Zn_3LH_2} = [Zn_3LH_2^{8+}] / [H^+][Zn_3LH^{7+}]$$



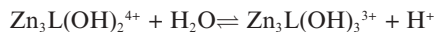
$$K_{Zn_3LH_3} = [Zn_3LH_3^{9+}] / [H^+][Zn_3LH_2^{8+}]$$



$$K_{Zn_3LOH} = [Zn_3L(OH)^{5+}][H^+] / [Zn_3L]$$



$$K_{Zn_3L(OH)_2} = ([Zn_3L(OH)_2^{4+}][H^+]) / [Zn_3L(OH)^{5+}]$$



$$K_{Zn_3L(OH)_3} = [Zn_3L(OH)_3^{3+}][H^+] / [Zn_3L(OH)_2^{4+}]$$

The occurrence of mononuclear and dinuclear species was also considered. Using such an extended equilibrium model for the curve-fitting procedure did not affect the overall standard deviation, which suggests that the formation of these species was negligible. This observation is consistent with the NMR spectral data of **7** in 50% (v/v) CH<sub>3</sub>CN–H<sub>2</sub>O wherein formation of mononuclear or dinuclear species was not observed even after two weeks. The results of the fitting allowed the calculation

of the stability constants of the trinuclear species [Zn<sub>3</sub>LH<sub>3</sub>]<sup>9+</sup>, [Zn<sub>3</sub>LH<sub>2</sub>]<sup>8+</sup>, [Zn<sub>3</sub>LH]<sup>7+</sup>, [Zn<sub>3</sub>L]<sup>6+</sup>, [Zn<sub>3</sub>L(OH)]<sup>5+</sup>, [Zn<sub>3</sub>L(OH)<sub>2</sub>]<sup>4+</sup> and [Zn<sub>3</sub>L(OH)<sub>3</sub>]<sup>3+</sup>. As often found in polyamine ligands with a large number of amine donors,<sup>64</sup> the mononuclear and dinuclear complexes display a marked tendency to add a third metal to give stable trinuclear Zn(II) species, which are largely prevalent in 50% (v/v) CH<sub>3</sub>CN–H<sub>2</sub>O solutions containing metal and ligand in a 3 : 1 molar ratio, Fig. 6. Though the species distribution diagram indicates the presence of various trinuclear zinc species in solution, the <sup>1</sup>H NMR spectra of **7** in 50% (v/v) CD<sub>3</sub>CN–D<sub>2</sub>O indicate a highly symmetric structure. This suggests that the proton exchange reaction between the various species is sufficiently fast in 50% (v/v) CD<sub>3</sub>CN–D<sub>2</sub>O on the NMR time scale.<sup>59</sup>

The formation of [Zn<sub>3</sub>L]<sup>6+</sup> species occurs at acidic pH and is followed by the formation of mono-, di- and trihydroxo complexes by successive deprotonation of the coordinated water molecules at slightly acidic to alkaline pH values. The structure of trihydroxo species, [Zn<sub>3</sub>L(OH)<sub>3</sub>]<sup>3+</sup> should correspond to the structure of the cation of **7** which was characterized by X-ray crystallography. In this complex, the metal displays a coordination environment not saturated by the ligand donors. All three zinc binding sites are occupied by tetrahedral zinc(II) ions coordinated by the pyridyl nitrogen and the piperazine nitrogen atoms from each arm of the ligand. The remaining two coordination sites of the zinc ion are filled by bridging hydroxides. The trinuclear Zn(II) species, [Zn<sub>3</sub>L]<sup>6+</sup> exhibited low p*K*<sub>a</sub> values for the formation of mono-, di- and trihydroxo trinuclear complexes (p*K*<sub>a1</sub> = 6.53, p*K*<sub>a2</sub> = 6.88, p*K*<sub>a3</sub> = 7.64). The first two p*K*<sub>a</sub> values are quite close to one another and differ by only 0.35 units. The p*K*<sub>a</sub> value for deprotonation of the first water molecule in the [Zn<sub>3</sub>L]<sup>6+</sup> trinuclear complex is very low. This behavior indicates a strong binding of the hydroxide ion in [Zn<sub>3</sub>L(OH)]<sup>5+</sup> and is generally ascribed to a bridging coordination mode of OH between two metal centres.<sup>40,47,52</sup> This hypothesis is corroborated by the crystal structure of the [Zn<sub>3</sub>L(OH)<sub>3</sub>]<sup>3+</sup> cation, Fig. 2, which shows three zinc ions connected to each other by three bridging hydroxides. The metal coordination spheres of the three metal centers are not fulfilled by the ligand donors. Therefore, they would provide efficient substrate binding and activation. At the same time, facile deprotonation of metal-bound water molecules occur from slightly acidic to neutral pH, giving rise to Zn–OH groups as potential nucleophiles in hydrolytic reactions. These features make the trinuclear Zn(II) complex **7** a promising hydrolytic agent.

It is not possible to determine reaction mechanism based solely on crystal structure data. Nevertheless, structural information, when combined with kinetic data, can be very powerful for solving reaction mechanisms.

### Transesterification of hydroxypropyl-*p*-nitrophenyl phosphate (HPNP)

Complex **7** is insoluble in pure water and hence CH<sub>3</sub>CN was added as a cosolvent.<sup>65</sup> The catalytic activity of the trinuclear zinc complex **7**, towards the transesterification of HPNP was studied in 50% CH<sub>3</sub>CN–80 mM aqueous buffer at 25 °C. The pH dependence for the transesterification of HPNP by **7** was studied in the pH range of 6.4 to 7.2 and the optimum pH for the reaction was found to be 6.7 (Fig. 7). The catalyst precipitated out of the reaction mixture above pH 7.4. At pH 6.7, 5 mM of **7** induces a 16 900

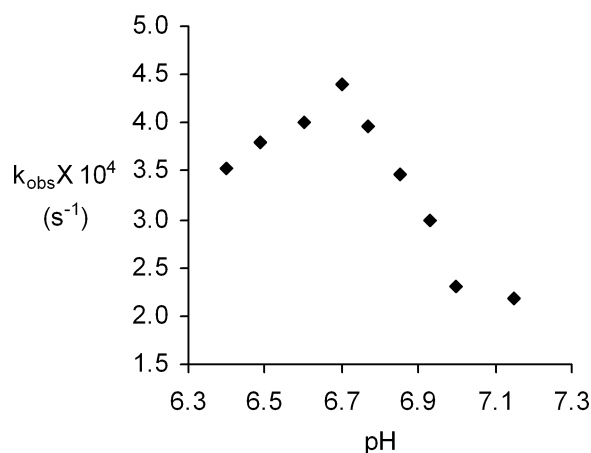


**Fig. 7** pH versus rate profile for transesterification of HPNP (2 mM) catalyzed by **7** (5 mM) in acetonitrile–80 mM buffer 1 : 1 (v/v) at 25 °C.

fold rate enhancement in the catalytic cyclization of the RNA model substrate, HPNP, compared to the uncatalyzed reaction, corresponding to a reduction of the half-life from approximately 308 d ( $k_{\text{uncat}} = (2.6 \pm 0.1) \times 10^{-8} \text{ s}^{-1}$ , error limits are given at the 95% confidence level unless otherwise stated)<sup>26,66</sup> for the uncatalyzed reaction to 26 min ( $k_{\text{obs}} = (4.4 \pm 0.1) \times 10^{-4} \text{ s}^{-1}$ ). The pH rate profile was then compared with the species distribution diagram (Fig. 6) in order to identify the reactive species. Since considerable concentration of  $[\text{Zn}_3\text{LH}]^{7+}$ ,  $[\text{Zn}_3\text{L}]^{6+}$ ,  $[\text{Zn}_3\text{L}(\text{OH})]^{5+}$  and  $[\text{Zn}_3\text{L}(\text{OH})_2]^{4+}$  are present in the solution, in the pH range 6.4 to 7.2, any or all of these might be the active species catalyzing the transesterification of HPNP. Thus, the optimum activity of the catalyst at pH 6.7 may not be due to the change in concentration of one particular species but is a consequence of the varying concentration of the different trinuclear zinc species.

The effect of concentration of **7** on the reaction rate was then investigated at pH 6.6. Within the concentration range explored (1.0 to 5.0 mM) the observed pseudo first order rate constant ( $k_{\text{obs}}$ ), for the transesterification of HPNP, exhibits a linear dependence on the concentration of the complex. The second order rate constant was determined as the slope of the linear plot of  $k_{\text{obs}}$  against catalyst concentration ( $k_2 = (7.9 \pm 0.2) \times 10^{-2} \text{ M}^{-1} \text{ s}^{-1}$ , Fig. 8).

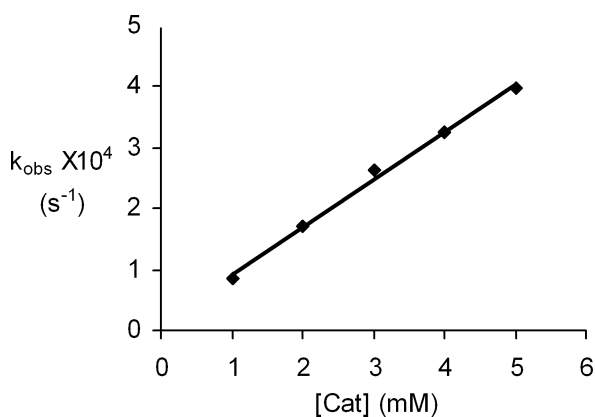


**Fig. 8** Dependence of the observed pseudo first order rate constant on the concentration of trinuclear zinc(II) catalyst **7** at pH 6.6 in 50%  $\text{CH}_3\text{CN}$ –80 mM MES buffer (v/v) at 25 °C.  $[\text{HPNP}] = 2 \text{ mM}$ .

The binding affinity of **7** towards HPNP was studied by measuring the rate of transesterification as a function of HPNP concentration, to investigate the catalytic process in more detail, at a fixed catalyst concentration. No saturation kinetics could be observed for **7** with up to 7 equivalents of HPNP (pH 6.6) indicating a low affinity for the substrate (Fig. 9). It is not possible to determine  $k_{\text{obs}}$  when  $[\text{Zn}(\text{ClO}_4)_2] \geq 0.8 \text{ mM}$  at pH 6.7 in the absence of ligand due to precipitation of Zn(II) hydroxide. With 0.4 mM  $\text{Zn}(\text{ClO}_4)_2$ , the value of  $k_{\text{obs}}$  was found to be  $(1.2 \pm 0.1) \times 10^{-6} \text{ s}^{-1}$ , indicating that the catalytic contribution of free Zn(II) towards the cleavage of HPNP in the presence of **7** is negligible.

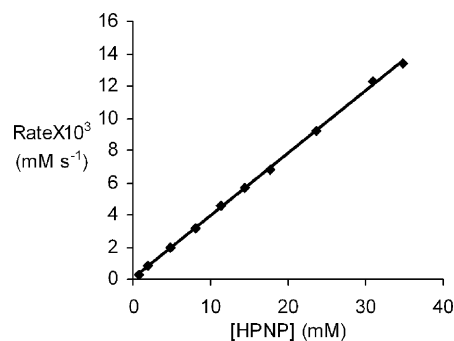


**Fig. 9** Initial rate as a function of the substrate concentration for the transesterification of HPNP.

To determine whether **7** acts as a catalyst for the transesterification of HPNP, reactions in the presence of 82 equivalents of the substrate were followed by  $^{31}\text{P}$  NMR spectroscopy. A progressive increase in the intensity of the signal corresponding to the cyclic phosphate ester with a simultaneous decrease of the HPNP signal was noted as outlined in Fig. 10. No other signal, including that of inorganic phosphate, was observed even after prolonged reaction times. In a separate experiment, catalytic turnover was demonstrated by preparing a reaction mixture consisting of 0.1 mM **7**, 2 mM HPNP and 80 mM MES buffer (pH 6.7). The absorbance at 400 nm produced by the release of *p*-nitrophenolate ion was monitored over a two day period and more than 10 turnovers of catalyst was noted. During the course of the multiple turnover reaction, the catalyst activity does decrease possibly due to product inhibition or catalyst decomposition as previously discussed.

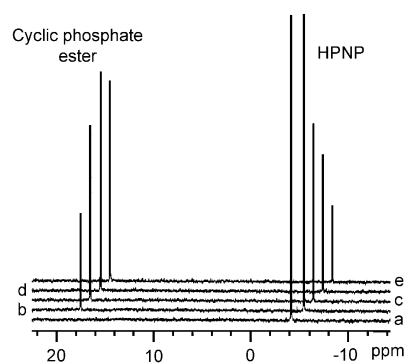


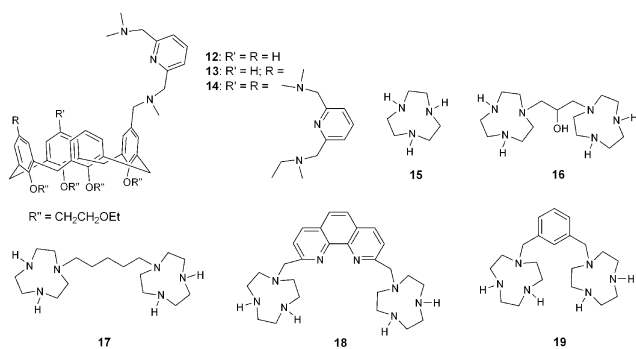
**Fig. 10** Stack plot of  $^{31}\text{P}$  NMR for the transesterification of HPNP (38.56 mM) catalyzed by **7** (0.47 mM) at pH 6.7 after (b) 1 d (c) 3 d (d) 5 d (e) 8 d. Spectrum (a) was taken before addition of the catalyst.

**Table 5** Rate constants for the transesterification of HPNP catalyzed by Zn(II) complexes at 25 °C

Catalyst <sup>a</sup>	pH	$k_2 \times 10^2 / \text{M}^{-1} \text{s}^{-1}$	Ref.
<b>7</b>	6.7	7.9	This work
Zn( <b>12</b> )	7.0	1.5	23
Zn <sub>2</sub> ( <b>13</b> )	7.0	4300	23
Zn <sub>2</sub> ( <b>13</b> )	7.4	1700	23
Zn <sub>3</sub> ( <b>14</b> )	7.0	290	23
Zn( <b>15</b> )	7.6	0.21	29
Zn <sub>2</sub> ( <b>16</b> )	7.6	25	29
Zn <sub>2</sub> ( <b>17</b> )	7.6	1.1	29
Zn <sub>2</sub> ( <b>18</b> )	7.6	0.89	29
Zn <sub>2</sub> ( <b>19</b> )	7.6	0.58	29

<sup>a</sup> For structures of these complexes see Fig. 11.

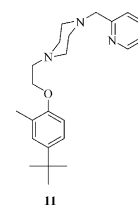
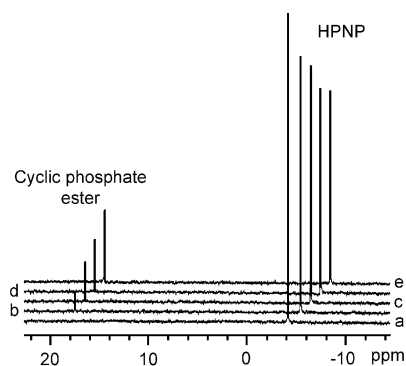
With ligands adept at forming trimetallic complexes, the orientation and flexibility of the metal binding groups impacts substrate binding. Reinhoudt and coworkers investigated the transesterification of HPNP catalyzed by the co-operative action of multiple Zn(II) centers tethered to the upper rim of a semi-flexible calix[4]arene.<sup>26,66</sup> The trizinc calix[4]arene complex exhibited saturation kinetics, and the second order rate constant,  $k_2$  for the transesterification of HPNP by this catalyst at pH 7 is  $2.9 \text{ M}^{-1} \text{ s}^{-1}$ . Strong substrate binding to the Zn(II) complex has the effect of increasing the second order rate constant. In the case of **7**, substrate binding appears to be impeded either by the crowded nature of the trinuclear cluster or possibly by the presence of bridging hydroxides between the metal centers, consequently, the value for  $k_2$  is low. The bound hydroxides may lower the substrate binding affinity of the catalyst by diminishing the Lewis acidity of the Zn(II) centers.<sup>40,47,52</sup> Nevertheless, once bound, HPNP is rapidly converted to the product by **7**. Table 5 summarizes the second order rate constants ( $k_2 / \text{M}^{-1} \text{ s}^{-1}$ ) for the transesterification of HPNP catalyzed by several different Zn(II) complexes (Fig. 11).

**Fig. 11** Structure of ligands mentioned in Table 5.

Although a remarkable rate of acceleration in the transesterification of HPNP has been observed, no significant activity for the cleavage of the internucleosidic phosphodiester bonds of diribonucleoside monophosphate diester has been found for complex **7** under a variety of conditions. These results indicate that stabilization of the leaving group indeed plays an important part in the hydrolytic cleavage of phosphate diester bonds in nucleotides like RNA and DNA. Moreover, the trinuclear cluster might be sterically too encumbered for the efficient substrate binding.

## Potential catalytic mechanisms

To facilitate a better insight into the mechanism, phosphodiesterase activity of the trinuclear zinc complex **7** was compared with that of a mononuclear zinc complex, prepared *in situ* by the addition of one equivalent of Zn(ClO<sub>4</sub>)<sub>2</sub>·6H<sub>2</sub>O to a solution of **11** (Fig. 12). A progressive increase in the intensity of the signal corresponding to the cyclic phosphate ester with a simultaneous decrease of the HPNP signal can be noted in Fig. 13. No other signal, including that of inorganic phosphate, was observed even after prolonged reaction times, indicating that the cyclic phosphate ester is not further hydrolyzed by the mononuclear zinc complex. The trinuclear Zn(II) catalyst exhibits a higher hydrolytic activity as compared to its mononuclear analogue as can be realized qualitatively by comparing Fig. 10 and Fig. 13. The mononuclear analog is, however, more active than free Zn(II) ions.

**Fig. 12** Structure of ligand **11**.**Fig. 13** Stack plot of <sup>31</sup>P NMR for the transesterification of HPNP (38.56 mM) catalyzed by a mixture of **11** (1.41 mM) and Zn(ClO<sub>4</sub>)<sub>2</sub>·6H<sub>2</sub>O (1.41 mM) at pH 6.7 after (b) 1 d (c) 3 d (d) 5 d (e) 8 d. Spectrum (a) was taken before addition of **11** and Zn(ClO<sub>4</sub>)<sub>2</sub>·6H<sub>2</sub>O.

In the trinuclear zinc complex, the three Zn(II) ions are kept in close proximity by use of a hydroxide bridging ligand.<sup>40,47,52</sup> The bridging hydroxide group presumably shields the electrostatic interactions between the Zn(II) ions and allows the cations to be drawn relatively close together in a complex of greatly enhanced activity. This high density of positive charge at **7** is ideal for providing electrostatic stabilization of the transition state for cleavage of HPNP relative to the reactant state because there is a net increase in negative charge on proceeding from the reactant to the transition state.

As discussed above, though any or all of the following species ([Zn<sub>3</sub>LH]<sup>7+</sup>, [Zn<sub>3</sub>L]<sup>6+</sup>, [Zn<sub>3</sub>L(OH)]<sup>5+</sup> and [Zn<sub>3</sub>L(OH)<sub>2</sub>]<sup>4+</sup>) might be the active species catalyzing the transesterification of HPNP, the pH-rate profiles for metal-ion catalyzed cleavage of RNA and RNA analogues frequently track the formation of metal ion

hydroxide complexes. A hydroxide (or water) spanning two zinc ions has been detected crystallographically in many hydrolases and is often considered as the active nucleophile, but it can be expected to exhibit rather low nucleophilicity if coordinated in a tightly bridging form.<sup>3,14,15,67</sup> Thus, it has been suggested that upon substrate binding a shift of the bridging hydroxide to a terminal position occurs prior to attack on the coordinated substrate.<sup>68,69</sup> As discussed above, in **7** three metal ions are held at a short distance, and at the same time, the ligand donors poorly saturate the coordination sphere of the metal ions. These structural features would favor a bridging interaction mode of the phosphate ester.<sup>70</sup> Substrate interaction with the electrophilic metal centers promotes the nucleophilic attack of a Zn–OH function and thus enhances the rate of hydrolytic process, as found in several synthetic Zn(II) complexes.<sup>23,26,71</sup> The  $\mu$ -1,3 bridged phosphoester unit has frequently been postulated as the preferred substrate binding mode in various metallophosphoesterases. A recent crystal structure of native *Escherichia coli* alkaline phosphatase complexed with inorganic phosphate shows the phosphate anions bridging the two Zn(II) ions, which lie 3.94 Å apart from each other.<sup>72–75</sup> Similarly, the X-ray crystal structure of the complex of PLC<sub>BC</sub> (phospholipase C from *Bacillus cereus*) with a competitive inhibitor (a phospholipid analog) revealed that the phosphate binds to all three Zn(II) ions by replacing two of the zinc-bound water molecules in the native PLC<sub>BC</sub>.<sup>13,76,77</sup>

Although **7** efficiently catalyzes the transesterification of HPNP, it is not catalytically active in the hydrolysis of ethyl *p*-nitrophenyl phosphate demonstrating that the  $\beta$ -hydroxyl group of HPNP is essential for hydrolysis. Based on the above discussion, the high activity in HPNP transesterification observed for our trinuclear Zn(II) complex may be explained by considering that the phosphate ester would interact with the Zn(II) centers, resulting in substrate activation. The subsequent facile intramolecular transesterification of the phosphate diester bond may either involve deprotonation of the hydroxy group by the bridging hydroxide that acts as a general base or the direct coordination of the substrate alcoholic function to the metal ion and the subsequent nucleophilic attack by the deprotonated hydroxy group of the substrate.<sup>78</sup>

## Conclusions

Inspired by trinuclear Zn sites in enzymatic systems, a  $C_3$ -symmetric trinuclear Zn(II) hydroxide complex of **5** was synthesized and fully characterized using NMR spectroscopy and X-ray crystallography. This complex at 5 mM concentration induces a 16900-fold rate enhancement in the catalytic cyclization of the RNA model substrate, 2-hydroxypropyl-*p*-nitrophenyl phosphate (HPNP, pH 6.7, 25 °C), over the uncatalyzed reaction with multiple catalyst turnovers.

On the time scale of the <sup>1</sup>H NMR spectra, a  $C_3$ -symmetric core is maintained in solution under the conditions used for the kinetic experiments (pH 6.7, 50% (v/v) CD<sub>3</sub>CN–D<sub>2</sub>O, buffer, [7] = 7.5 mM) but there may be various trinuclear zinc species in solution at and around pH 6.7 as depicted by the species distribution diagram. The proton exchange reaction between the various species appears to be sufficiently fast in 50% (v/v) CD<sub>3</sub>CN–D<sub>2</sub>O on the NMR time scale and thus some sort of hydroxide bridged  $C_3$ -symmetric species was observed.

The trinuclear Zn(II) complex exhibits a higher hydrolytic activity as compared to its mononuclear analogue. Although **7** efficiently catalyzes the transesterification of HPNP, it is not catalytically active in the hydrolysis of ethyl *p*-nitrophenyl phosphate demonstrating that the  $\beta$ -hydroxyl group of HPNP is essential for hydrolysis. Based on the experimental observations, the metal catalyzed facile intramolecular transesterification of HPNP may either involve the participation of the bridging hydroxide as a general base or the nucleophilic attack by the deprotonated hydroxy group of the substrate.

## Experimental

### General methods

All reagents and solvents were of analytical grade and were used without purification, unless otherwise noted. Aqueous solutions were prepared using 18 M $\Omega$  Millipore deionized water. 4-*tert*-butyl-2-methylphenol, 2-morpholinoethanesulfonic acid (MES), *N*-(2-hydroxyethyl)piperazine-*N'*-(2-ethanesulfonic acid) (HEPES) and Zn(II) perchlorate hexahydrate were purchased from Sigma–Aldrich. The barium salt of 2-hydroxypropyl-4-nitrophenyl phosphate (HPNP)<sup>79</sup> and 1-[(2-pyridyl)methyl]piperazine<sup>80</sup> were prepared following literature methods. All <sup>1</sup>H, <sup>13</sup>C and <sup>31</sup>P NMR spectra were recorded on a Varian VXR-300 or Mercury-300 spectrometer at 299.95, 75.4 and 121.42 MHz for the proton, carbon and phosphorus channels, respectively. Elemental analyses were performed by Complete Analysis Laboratories, Inc. in Parsippany, NJ. IR spectra were recorded as KBr discs on a Bruker Vector-22 instrument at a resolution of 2 cm<sup>-1</sup>. The pH meter used for adjustment of buffered solution was calibrated daily.

### Synthesis of the compounds

Detailed synthesis of **8**, **9**, **10** and **11** are reported in the ESI†.

#### Tris(3-methyl-5-*tert*-butylphenoxy)methane (**1**)

Using an aldehyde condensation method for tris(3,5-*tert*-butyl-2-hydroxyphenyl)methane,<sup>54,81</sup> a 50 mL methanol solution of 10.66 g (64.9 mmol) of 2-methyl-4-*tert*-butylphenol, and 5.33 g (27.7 mmol) 2-carboxaldehyde-6-methyl-4-*tert*-butylphenol, chilled to 0° C in an ice bath was acidified to saturation with ~25 mL of thionyl chloride. The solution was allowed to warm up to room temperature and then stirred overnight, during which an off-white product, **1**, precipitated from the solution. The solid was filtered from the reaction mixture and washed with methanol to afford 9.68 g (70%) of clean **1**. IR:  $\nu$  [cm<sup>-1</sup>] 3454 (O–H). <sup>1</sup>H NMR ((CD<sub>3</sub>)<sub>2</sub>SO):  $\delta$  = 1.08 (s, 27 H, Ar–C(CH<sub>3</sub>)<sub>3</sub>), 2.11 (s, 9 H, Ar–CH<sub>3</sub>), 6.60 (s, 1 H, CH), 6.70 (d, <sup>4</sup>*J*(H,H) = 1.9 Hz, 3 H, Ar–*H*), 6.84 (d, <sup>4</sup>*J*(H,H) = 1.9 Hz, 3 H, Ar–*H*). <sup>13</sup>C NMR ((CD<sub>3</sub>)<sub>2</sub>SO):  $\delta$  = 17.2 (Ar–C(CH<sub>3</sub>)<sub>3</sub>), 31.3 (Ar–C(CH<sub>3</sub>)<sub>3</sub>), 33.5 (Ar–CH<sub>3</sub>), 36.0 (CH), 123.2, 124.5, 124.6, 130.7, 140.0, 150.0 (Ar). Elemental anal. Found: C, 81.09; H, 9.07. Calcd. for C<sub>34</sub>H<sub>46</sub>O<sub>3</sub>: C, 81.23; H, 9.22.

#### Tris(2-ethylacetoxy-3-methyl-5-*tert*-butylphenyl)methane (**2**)

Following a previously published method for the preparation of tris(3,5-di-*tert*-butyl-2-ethoxycarbonylmethoxyphenyl)

methane,<sup>54,81</sup> in a Schlenk flask under argon 0.56 g (1.1 mmol) of **1** was dissolved in dry acetone and 0.61 g (3.7 mmol) of ethyl bromoacetate and 1.43 g (4.4 mmol) of Cs<sub>2</sub>CO<sub>3</sub> was added. The mixture was refluxed for 12–15 h and then cooled to room temperature. The acetone was removed under vacuum and the solids dissolved in diethyl ether. Solid MgSO<sub>4</sub> was added and the insoluble salts and drying agent were filtered off. The ether was removed from the filtrate to give the crude product. The white solid was recrystallized in ethanol to give 0.72 g (85%) of product. IR:  $\nu$  [cm<sup>-1</sup>] 1725 (C=O). <sup>1</sup>H NMR (CDCl<sub>3</sub>):  $\delta$  = 1.14 (s, 27 H, Ar-C(CH<sub>3</sub>)<sub>3</sub>), 1.30 (t, <sup>3</sup>J(H,H) = 7.1 Hz, 9 H, COOCH<sub>2</sub>CH<sub>3</sub>), 2.23 (s, 9 H, Ar-CH<sub>3</sub>), 4.16 (s, 6 H, Ar-O-CH<sub>2</sub>-COOEt), 4.23 (q, <sup>3</sup>J(H,H) = 7.1 Hz, 6 H, COOCH<sub>2</sub>CH<sub>3</sub>), 6.48 (s, 1 H, CH), 6.72 (d, <sup>4</sup>J(H,H) = 2.4 Hz, 3 H, Ar-H), 6.99 (d, <sup>4</sup>J(H,H) = 2.4 Hz, 3 H, Ar-H). <sup>13</sup>C NMR (CDCl<sub>3</sub>):  $\delta$  = 14.1 (OCH<sub>2</sub>CH<sub>3</sub>), 16.6 (Ar-CH<sub>3</sub>), 31.3 (Ar-C(CH<sub>3</sub>)<sub>3</sub>), 34.1 (Ar-C(CH<sub>3</sub>)<sub>3</sub>), 38.1 (C-H), 61.0 (OCH<sub>2</sub>CH<sub>3</sub>), 69.5 (Ar-O-CH<sub>2</sub>-COOEt), 125.7, 126.4, 129.8, 135.4, 146.1, 152.4 (Ar), 169.2 (C=O). Elemental anal. Found: C, 72.49; H, 8.54. Calcd. for C<sub>46</sub>H<sub>64</sub>O<sub>9</sub>: C, 72.60; H, 8.48.

#### Tris[2-(2-hydroxyethoxy)-3-methyl-5-*tert*-butylphenyl]methane (**3**)

A dry diethyl ether solution of **2** (1.47 g, 1.9 mmol) was added dropwise over 1–2 h with an addition funnel to a slurry of LiAlH<sub>4</sub> (0.44 g, 11.7 mmol) in 100 mL dry diethyl ether cooled to 0° C. The mixture was then warmed to room temperature and stirred 12–15 h. The excess reductant was destroyed with 1 M HCl (100 mL). The ether layer was separated and further extracted with 1 M HCl (2 × 100 mL) and brine (100 mL). The ether was then dried with MgSO<sub>4</sub>. After filtration of the drying agent, the ether was removed to give 1.06 g (88%) of white crystalline material. IR:  $\nu$  [cm<sup>-1</sup>] 3454 (OH). <sup>1</sup>H NMR (CDCl<sub>3</sub>):  $\delta$  = 1.18 (s, 27 H, Ar-C(CH<sub>3</sub>)<sub>3</sub>), 2.25 (s, 9 H, Ar-CH<sub>3</sub>), 3.79 (t, <sup>3</sup>J(H,H) = 7.8 Hz, 6 H, Ar-O-CH<sub>2</sub>), 3.84 (m, 6 H, Ar-O-CH<sub>2</sub>CH<sub>2</sub>OH), 4.06 (t, <sup>3</sup>J(H,H) = 5.5 Hz, 3 H, CH<sub>2</sub>CH<sub>2</sub>OH), 6.79 (s, 1 H, CH), 6.92 (d, <sup>4</sup>J(H,H) = 2.4 Hz, 3 H, Ar-H), 7.01 (d, <sup>4</sup>J(H,H) = 2.4 Hz, 3 H, Ar-H). <sup>13</sup>C NMR (CDCl<sub>3</sub>):  $\delta$  = 16.9 (Ar-CH<sub>3</sub>), 31.3 (Ar-C(CH<sub>3</sub>)<sub>3</sub>), 34.1 (Ar-C(CH<sub>3</sub>)<sub>3</sub>), 36.7 (C-H), 62.0 (Ar-O-CH<sub>2</sub>CH<sub>2</sub>OH), 74.0 (Ar-O-CH<sub>2</sub>CH<sub>2</sub>OH), 125.5, 126.1, 129.8, 135.8, 145.7, 152.0 (Ar). Elemental anal. Found: C, 75.50; H, 9.25. Calcd for C<sub>40</sub>H<sub>58</sub>O<sub>6</sub>: C, 75.67; H, 9.21.

#### Tris[2-(2-toluenesulfonyloxy)-3-methyl-5-*tert*-butylphenyl]methane (**4**)

In a dry flask 3.83 g (6 mmol) of **3** was dissolved in 100 mL of dry pyridine and cooled to 0° C in an ice bath. A 4.58 g (24 mmol) portion of toluene sulfonyl chloride was added and the reaction mixture was stirred for 2 h at 0° C and then for 12–15 h at room temperature. The pyridine was removed under vacuum and the solid material dissolved in 100 mL methylene chloride and then extracted with 1 M HCl (2 × 100 mL). The organic phase was then dried with MgSO<sub>4</sub>, filtered, and the solvent removed. Methanol was added and the white solid product filtered off and washed with more dry methanol to afford 5.35 g (74%) product. <sup>1</sup>H NMR (CDCl<sub>3</sub>):  $\delta$  = 1.14 (s, 27 H, Ar-C(CH<sub>3</sub>)<sub>3</sub>), 2.13 (s, 9 H, Ar-CH<sub>3</sub>), 2.42 (s, 3 H, SO<sub>2</sub>Ar-CH<sub>3</sub>), 3.49 (t, 6 H, <sup>3</sup>J(H,H) = 6.0 Hz, Ar-O-CH<sub>2</sub>), 4.14 (t, 6 H, <sup>3</sup>J(H,H) = 6.0 Hz, Ar-O-CH<sub>2</sub>CH<sub>2</sub>), 6.45 (s, 1

H, CH), 6.83 (d, <sup>4</sup>J(H,H) = 2.4 Hz, 3 H, Ar-H), 6.95 (d, <sup>4</sup>J(H,H) = 2.4 Hz, 3 H, Ar-H), 7.32 (d, <sup>3</sup>J(H,H) = 8.1 Hz, 6 H, SO<sub>2</sub>Ar-H), 7.78 (d, <sup>3</sup>J(H,H) = 8.1 Hz, 6 H, SO<sub>2</sub>Ar-H). <sup>13</sup>C NMR (CDCl<sub>3</sub>):  $\delta$  = 16.5 (Ar-CH<sub>3</sub>), 21.6 (SO<sub>2</sub>Ar-CH<sub>3</sub>), 31.3 (Ar-C(CH<sub>3</sub>)<sub>3</sub>), 34.1 (Ar-C(CH<sub>3</sub>)<sub>3</sub>), 36.8 (C-H), 69.5 (Ar-O-CH<sub>2</sub>CH<sub>2</sub>), 69.6 (Ar-O-CH<sub>2</sub>CH<sub>2</sub>), 125.4, 126.2, 127.9, 129.9, 130.1, 133.0, 135.8, 144.7, 146.1, 151.9 (Ar). Elemental anal. Found: C, 66.77; H, 6.96. Calcd for C<sub>61</sub>H<sub>76</sub>O<sub>12</sub>S<sub>3</sub>: C, 66.76; H, 6.98.

#### Preparation of tris[2-{2-[4-[(2-pyridyl)methyl]piperazine]-1-ethoxy}-3-methyl-5-*tert*-butylphenyl]methane (**5**)

To 0.74 g (0.61 mmol) of **4** dissolved in 50 mL dry acetonitrile was added 3.2 g (18.2 mmol) of 1-[(2-pyridyl)methyl]piperazine, and 0.64 g (6.1 mmol) of Na<sub>2</sub>CO<sub>3</sub>, and the mixture was refluxed for 5 d under an inert atmosphere. The solvent was then removed under vacuum and the remaining material dissolved in diethyl ether. The organic layer was extracted with 0.1 M NaOH (2 × 100 mL), then dried with Na<sub>2</sub>SO<sub>4</sub>, filtered, and the solvent removed to afford 0.62 g (91%) of the brownish–yellow amorphous solid. The excess 1-[(2-pyridyl)methyl]piperazine was recovered from the aqueous phase by extraction with chloroform and removing the solvent under vacuum. Slow diffusion of pentane into a concentrated tetrahydrofuran solution of ligand at –30° C afforded crystals suitable for X-ray analysis. <sup>1</sup>H NMR (CD<sub>3</sub>CN):  $\delta$  = 1.12 (s, 27 H, Ar-C(CH<sub>3</sub>)<sub>3</sub>), 2.21 (s, 9 H, Ar-CH<sub>3</sub>), 2.39 (b, 24 H, N-CH<sub>2</sub>CH<sub>2</sub>-N), 2.57 (t, <sup>3</sup>J(H,H) = 6.3 Hz, 6 H, Ar-O-CH<sub>2</sub>CH<sub>2</sub>N), 3.52 (t, <sup>3</sup>J(H,H) = 6.3 Hz, 6 H, Ar-O-CH<sub>2</sub>), 3.56 (s, 6 H, Py-CH<sub>2</sub>), 6.52 (s, 1 H, CH), 6.78 (d, <sup>4</sup>J(H,H) = 2.4 Hz, 3 H, Ar-H), 7.07 (d, <sup>4</sup>J(H,H) = 2.1 Hz, 3 H, Ar-H), 7.17 (ddd, <sup>3</sup>J(H,H) = 7.7 Hz, <sup>4</sup>J(H,H) = 5.0 Hz, <sup>5</sup>J(H,H) = 1.2 Hz, 3 H, Py), 7.40 (m, 3 H, Py), 7.68 (dt, <sup>3</sup>J(H,H) = 7.7 Hz, <sup>4</sup>J(H,H) = 2.0 Hz, 3 H, Py), 8.47 (ddd, <sup>3</sup>J(H,H) = 5.4 Hz, <sup>4</sup>J(H,H) = 1.7 Hz, <sup>5</sup>J(H,H) = 0.9 Hz, 3 H, Py). <sup>13</sup>C NMR (CD<sub>3</sub>CN):  $\delta$  = 17.1 (Ar-CH<sub>3</sub>), 31.8 (Ar-C(CH<sub>3</sub>)<sub>3</sub>), 34.8 (Ar-C(CH<sub>3</sub>)<sub>3</sub>), 38.8 (C-H), 54.2 (Ar-O-CH<sub>2</sub>CH<sub>2</sub>-N-CH<sub>2</sub>), 54.6 (CH<sub>2</sub>-N-CH<sub>2</sub>-Py), 58.7 (Ar-O-CH<sub>2</sub>CH<sub>2</sub>), 65.2 (N-CH<sub>2</sub>-Py), 71.0 (Ar-O-CH<sub>2</sub>), 123.0 (Py), 123.8 (Py), 126.5 (Ar), 127.0 (Ar), 131.2 (Ar), 137.3 (Ar), 137.5 (Py), 146.4 (Ar), 149.9 (Py), 154.2 (Ar), 160.0 (Py). Elemental anal. Found: C, 73.14; H, 9.16; N, 10.72. Calcd. for **5**·2H<sub>2</sub>O (C<sub>70</sub>H<sub>101</sub>N<sub>9</sub>O<sub>8</sub>): C, 73.20; H, 8.86; N, 10.98. ESI FT-ICR MS *m/z* = 1112.78 [M + H]<sup>+</sup>.

#### Preparation of hydrochloride salt of tris[2-{2-[4-[(2-pyridyl)methyl]piperazine]-1-ethoxy}-3-methyl-5-*tert*-butylphenyl]methane (**6**)

The HCl salt of **5** (tris[2-{2-[4-[(2-pyridyl)methyl]piperazine]-1-ethoxy}-3-methyl-5-*tert*-butylphenyl]methane) was prepared by dissolving it in diethyl ether and adding 2 N HCl in diethyl ether resulting in the formation of a white precipitate, which is thoroughly washed with diethyl ether and dried under vacuum. The product formed was **5**·HCl·4H<sub>2</sub>O·Et<sub>2</sub>O. <sup>1</sup>H NMR (D<sub>2</sub>O):  $\delta$  = 1.02 (s, 27 H, Ar-C(CH<sub>3</sub>)<sub>3</sub>), 2.31 (s, 9 H, Ar-CH<sub>3</sub>), 3.05–4.19 (m, 42 H), 6.60 (s, 1 H, CH), 6.64 (s, 3 H, Ar-H), 7.21 (s, 3 H, Ar-H), 8.04 (m, 6 H, Py), 8.57 (dt, <sup>3</sup>J(H,H) = 7.95 Hz, <sup>4</sup>J(H,H) = 1.5 Hz, 3 H, Py), 8.77 (d, <sup>4</sup>J(H,H) = 5.4 Hz, 3 H, Py). <sup>13</sup>C NMR (D<sub>2</sub>O):  $\delta$  = 16.87 (Ar-CH<sub>3</sub>), 31.19 (Ar-C(CH<sub>3</sub>)<sub>3</sub>), 34.07 (Ar-C(CH<sub>3</sub>)<sub>3</sub>), 49.11 (C-H), 50.85 (Ar-O-CH<sub>2</sub>-CH<sub>2</sub>-N-CH<sub>2</sub>), 52.04

(CH<sub>2</sub>-N-CH<sub>2</sub>-Py), 56.07 (Ar-O-CH<sub>2</sub>-CH<sub>2</sub>), 57.1 (N-CH<sub>2</sub>-Py), 65.52 (Ar-O-CH<sub>2</sub>), 125.61 (Py), 126.49 (Py), 127.23 (Ar), 127.58 (Ar), 128.44 (Ar), 130.87 (Ar), 135.98 (Py), 141.58 (Ar), 147.2 (Py), 152.1 (Ar), 152.37 (Py). Elemental anal. Found: C, 55.75; H, 8.13; N, 8.29. Calcd. for 5·9HCl·4H<sub>2</sub>O·Et<sub>2</sub>O (C<sub>74</sub>H<sub>124</sub>Cl<sub>9</sub>N<sub>9</sub>O<sub>8</sub>): C, 56.01; H, 7.88; N, 7.94. The presence of nine HCl molecules per molecule of the ligand is further supported by the observation that nine equivalents of KOH are required to completely neutralize one equivalent of the protonated ligand, **6**, as depicted in Fig. 5 (*vide supra*).

### Preparation of [5·Zn<sub>3</sub>(μ-OH)<sub>3</sub>](ClO<sub>4</sub>)<sub>3</sub> (**7**)

(**Caution!** Although, the perchlorate salt is moderately stable, it is a potential hazard and should therefore be handled with care.) **5** (20 mg, 0.018 mmol) was dissolved in 1 mL acetone and added to a solution of Zn(ClO<sub>4</sub>)<sub>2</sub>·6H<sub>2</sub>O (20.11 mg, 0.054 mmol) in 1 mL of acetone mixed with a few drops of methanol (to dissolve Zn(ClO<sub>4</sub>)<sub>2</sub>·6H<sub>2</sub>O completely). Diffusion of pentane at 0 °C into the above solution afforded colorless crystals suitable for X-ray analysis. Isolated yield (17.9 mg, 60%). <sup>1</sup>H NMR (CD<sub>3</sub>CN): δ = 1.20 (s, 27 H, Ar-C(CH<sub>3</sub>)<sub>3</sub>), 2.20 (s, 3 H, O-H), 2.29 (s, 9 H, Ar-CH<sub>3</sub>), 2.6–3.7 (b, 36 H, N-CH<sub>2</sub>-CH<sub>2</sub>-N & Ar-O-CH<sub>2</sub>CH<sub>2</sub>N), 4.17 (s, 6 H, Py-CH<sub>2</sub>), 7.10 (s, 1 H, CH), 7.12 (d, <sup>4</sup>J(H,H) = 2.4 Hz, 3 H, Ar-H), 7.20 (d, <sup>4</sup>J(H,H) = 2.4 Hz, 3 H, Ar-H), 7.70 (m, 6 H, Py), 8.20 (dt, <sup>3</sup>J(H,H) = 7.7 Hz, <sup>4</sup>J(H,H) = 1.8 Hz, 3 H, Py), 8.80 (d, <sup>3</sup>J(H,H) = 5.1 Hz, 3 H, Py). <sup>13</sup>C NMR (CD<sub>3</sub>CN): δ = 16.8 (Ar-CH<sub>3</sub>), 31.7 (Ar-C(CH<sub>3</sub>)<sub>3</sub>), 34.9 (Ar-C(CH<sub>3</sub>)<sub>3</sub>), 35.6 (C-H), 55.6 (Ar-O-CH<sub>2</sub>-CH<sub>2</sub>-N-CH<sub>2</sub>), 55.8 (CH<sub>2</sub>-N-CH<sub>2</sub>-Py), 58.3 (Ar-O-CH<sub>2</sub>-CH<sub>2</sub>), 63.0 (N-CH<sub>2</sub>-Py), 74.8 (Ar-O-CH<sub>2</sub>), 125.9 (Ar), 126.2 (Py), 126.9 (Ar), 131.5 (Ar), 137.2 (Ar), 143.2 (Py), 147.1 (Ar), 150.5 (Py), 153.4 (Ar), 155.1 (Py). Elemental anal. Found: C, 49.70; H, 5.99; N, 7.42; Cl, 6.24. Calcd. for 7·2H<sub>2</sub>O (C<sub>70</sub>H<sub>104</sub>N<sub>9</sub>O<sub>20</sub>Cl<sub>3</sub>Zn<sub>3</sub>): C, 49.63; H, 6.19; N, 7.44; Cl, 6.28.

### X-Ray crystallography†

Unit cell dimensions and intensity data for all the structures were obtained on a Siemens CCD SMART diffractometer at 173 K. The data collections nominally covered a hemisphere of reciprocal space, by a combination of three sets of exposures; each set had a different φ angle for the crystal, and each exposure covered 0.3° in ω. The crystal to detector distance was 5.0 cm. The data sets were corrected for absorption using SADABS.<sup>82</sup>

All the structures were solved using the Bruker SHELXTL software package for the PC, using the direct methods option of SHELXS. The space groups for the structures were determined from an examination of the systematic absences in the data, and the successful solution and refinement of the structures confirmed these assignments. All hydrogen atoms were assigned idealized locations and were given a thermal parameter equivalent to 1.2 to 1.5 times the thermal parameter of the atom to which it was attached. For the methyl groups, where the location of hydrogen atoms was uncertain, the AFIX 137 card was used to allow the hydrogen atoms to rotate to the maximum area of residual density, while fixing their geometry. Structural and refinement data for **5** and **7** are presented in Table 6.

**Table 6** Crystal data<sup>a</sup> and structure refinement for **5** and **7**

	5·C <sub>4</sub> H <sub>8</sub> O	7·3(CH <sub>3</sub> ) <sub>2</sub> CO
Formula <sup>a</sup>	C <sub>74</sub> H <sub>105</sub> N <sub>9</sub> O <sub>4</sub>	C <sub>79</sub> H <sub>109</sub> Cl <sub>3</sub> N <sub>9</sub> O <sub>21</sub> Zn <sub>3</sub>
Fw/g mol <sup>-1a</sup>	1184.67	1823.21
Space group	R $\bar{3}$ c	P $\bar{3}$
a/Å	16.7988(5)	16.7532(16)
b/Å	16.7988(5)	16.7532(16)
c/Å	102.377(4)	23.629(3)
V/Å <sup>3</sup>	25020.1(15)	5743.4(11)
Z	12	2
μ/mm <sup>-1</sup>	0.059	0.747
R <sub>1</sub> <sup>b</sup>	0.0805	0.0849
wR <sub>2</sub> <sup>c</sup>	0.2202	0.2355

<sup>a</sup> Obtained with monochromatic Mo-K radiation (λ = 0.71073 Å) at 173 K.  
<sup>b</sup> R<sub>1</sub> = Σ(|F<sub>o</sub> - |F<sub>c</sub>||) / Σ |F<sub>o</sub>|. <sup>c</sup> wR<sub>2</sub> = [Σ[w(F<sub>o</sub><sup>2</sup> - F<sub>c</sub><sup>2</sup>)<sup>2</sup>] / Σ[w(F<sub>o</sub><sup>2</sup>)<sup>2</sup>]]<sup>1/2</sup>, w = 1/[σ<sup>2</sup>(F<sub>o</sub><sup>2</sup>) + [(ap)<sup>2</sup> + bp]], where p = [F<sub>o</sub><sup>2</sup> + 2F<sub>c</sub><sup>2</sup>]/3.

### Potentiometric titrations

Potentiometric titrations were conducted in 50% (v/v) CH<sub>3</sub>CN-H<sub>2</sub>O mixture at an ionic strength of 0.1 M KCl with a Metrohm 702SM titrator equipped with a Metrohm combined pH glass electrode. The electrode system was calibrated before each measurement by titrating a known amount of HCl in the solvent mixture with a known concentration of KOH. The base solution with a concentration of ca. 0.1 M was made in the above solvent mixture and standardized using potassium hydrogen phthalate.<sup>83</sup> A plot of millivolts (measured) vs. pH (calculated) gave a working slope and intercept so that pH could be read as -log[H<sup>+</sup>] directly. The pK<sub>w</sub> value in 50% (v/v) CH<sub>3</sub>CN-H<sub>2</sub>O was determined to be 15.19 at 25 °C and is in good agreement with the published value.<sup>84</sup> The electrode was stored in solvent mixture between measurements.

All solutions were prepared with purified CH<sub>3</sub>CN and freshly boiled 18 MΩ Millipore deionized water cooled in a nitrogen stream. All solutions were carefully protected from air by a stream of nitrogen gas. The linearity of electrode response and carbonate contamination of the standardized KOH solution was determined by Gran's method and was found to be less than 2%.<sup>63,64,85,86</sup> The stock solution of Zn(II) (0.02 M) was prepared by dissolving Zn(ClO<sub>4</sub>)<sub>2</sub>·6H<sub>2</sub>O in 50% (v/v) CH<sub>3</sub>CN-H<sub>2</sub>O. This material was standardized with EDTA using Eriochrome Black T as indicator. The potentiometric titration of **6** (0.92 mM) in the absence and presence of 1, 2 and 3 equivalents of Zn(II) respectively were carried out at 25 °C with I = 0.1 M (KCl) under a nitrogen atmosphere. The equilibrium constants were calculated using the program BEST.<sup>63</sup> All σ fit values (as defined in the program) were smaller than 0.025. Species distribution was calculated using the program SPE.<sup>63</sup> At least two titration experiments (each with approximately 100 data points) were performed. The stepwise constants are denoted by K while the overall constants are denoted by β.

### Kinetic measurements

UV-Vis spectra and kinetic traces were recorded with a diode array spectrometer equipped with a thermostated multicell cuvette holder (7 cuvettes, 1.0 cm path length) (Hewlett Packard 8453). Solutions for kinetic measurements were made by adding CH<sub>3</sub>CN

(spectrophotometric grade) upto 50% (v/v) to a 80 mM aqueous buffer solution adjusted with NaOH to the desired pH. Buffers (MES, pH 5.6–7.0 and HEPES, pH 7.0–8.2) were obtained from commercial sources and used without further purification in 18 MΩ Millipore deionized water. Stock solutions were freshly prepared before performing the kinetic measurements. In a typical experiment, preformed complex **7** (1040 μL, 10 mM in CH<sub>3</sub>CN) was added to a cuvette containing 38 μL of CH<sub>3</sub>CN and 962.4 μL of 173.25 mM aqueous buffer solution and thermostated at 25 °C. After a couple of minutes of equilibration time, HPNP (41.6 μL, 100 mM in water) was injected and an increase in the UV absorption at  $\lambda = 400$  nm due to the release of *p*-nitrophenolate ion was recorded. All solutions remained clear during the time of the kinetic measurements. In the absence of ligand, precipitation of polymeric Zn(II) hydroxide took place. The observed pseudo-first-order rate constants  $k_{\text{obs}}$  (s<sup>-1</sup>) were calculated with the extinction coefficient of *p*-nitrophenolate at  $\lambda = 400$  nm by the initial slope method (<5% conversion). The method of initial rates was used to study these reactions as the catalyst was not stable for even one complete half-life of the reaction in the presence of excess buffer. Solutions of *p*-nitrophenolate in CH<sub>3</sub>CN–20 mM buffer 1 : 1 (v/v) were prepared at various pH values. The molar extinction coefficient for *p*-nitrophenolate at 400 nm was then determined from the plot of absorbance against concentration. Correction for the spontaneous hydrolysis of HPNP (less than 0.1%) was accomplished by direct observation of the production of *p*-nitrophenolate relative to a reference cell containing no metal complex. The pseudo-first-order rate constants for the transesterification of HPNP in the absence of the catalyst ( $k_{\text{uncat}}/s^{-1}$ ) were measured with a 2.0 mM HPNP solution by the method of initial rates. Each experiment was run in triplicate. Agreement between the calculated initial rates for replicate experiments was within 5%.

## Acknowledgements

We thank the National Science Foundation (Grant CHE-0316003) for funding this research. We are especially grateful to Professor David E. Richardson and Dr Kathryn R. Williams at the University Of Florida for the use of instruments and for helpful discussions. We also thank Daniel E. Denevan for his help with the UV experiments.

## References

- 1 F. H. Westheimer, *Science*, 1987, **235**, 1173.
- 2 N. H. Williams, B. Takasaki, M. Wall and J. Chin, *Acc. Chem. Res.*, 1999, **32**, 485.
- 3 N. Strater, W. N. Lipscomb, T. Klabunde and B. Krebs, *Angew. Chem., Int. Ed. Engl.*, 1996, **35**, 2024.
- 4 D. E. Wilcox, *Chem. Rev.*, 1996, **96**, 2435.
- 5 J. A. Cowan, *Chem. Rev.*, 1998, **98**, 1067.
- 6 M. J. Jedrzejas and P. Setlow, *Chem. Rev.*, 2001, **101**, 607.
- 7 M. M. Benning, H. Shim, F. M. Raushel and H. M. Holden, *Biochemistry*, 2001, **40**, 2712.
- 8 H. Shim and F. M. Raushel, *Biochemistry*, 2000, **39**, 7357.
- 9 E. E. Kim and H. W. Wyckoff, *J. Mol. Biol.*, 1991, **218**, 449.
- 10 B. Stec, K. M. Holtz and E. R. Kantrowitz, *J. Mol. Biol.*, 2000, **299**, 1303.
- 11 S. Hansen, L. K. Hansen and E. Hough, *J. Mol. Biol.*, 1993, **231**, 870.
- 12 S. Hansen, L. Kristian, H. Hough and E. Hough, *J. Mol. Biol.*, 1992, **225**, 543.

- 13 E. Hough, L. K. Hansen, B. Birknes, K. Jynge, S. Hansen, A. Hordvik, C. Little, E. Dodson and Z. Derewenda, *Nature*, 1989, **338**, 357.
- 14 C. Romier, R. Dominguez, A. Lahm, O. Dahl and D. Suck, *Proteins*, 1998, **32**, 414.
- 15 A. Volbeda, A. Lahm, F. Sakiyama and D. Suck, *EMBO J.*, 1991, **10**, 1607.
- 16 C. G. Zhan and F. Zheng, *J. Am. Chem. Soc.*, 2001, **123**, 2835.
- 17 Z. G. Wang, W. Fast and S. J. Benkovic, *Biochemistry*, 1999, **38**, 10013.
- 18 E. L. Hegg and J. N. Burstyn, *Coord. Chem. Rev.*, 1998, **173**, 133.
- 19 J. Weston, *Chem. Rev.*, 2005, **105**, 2151.
- 20 G. Parkin, *Chem. Rev.*, 2004, **104**, 699.
- 21 J. R. Morrow and O. Iranzo, *Curr. Opin. Chem. Biol.*, 2004, **8**, 192.
- 22 E. Kimura, *Curr. Opin. Chem. Biol.*, 2000, **4**, 207.
- 23 P. Molenveld, J. F. J. Engbersen and D. N. Reinhoudt, *Chem. Soc. Rev.*, 2000, **29**, 75.
- 24 M. Komiyama and J. Sumaoka, *Curr. Opin. Chem. Biol.*, 1998, **2**, 751.
- 25 R. Breslow, *Acc. Chem. Res.*, 1995, **28**, 146.
- 26 P. Molenveld, W. M. G. Stikvoort, H. Kooijman, A. L. Spek, J. F. J. Engbersen and D. N. Reinhoudt, *J. Org. Chem.*, 1999, **64**, 3896.
- 27 P. Molenveld, S. Kapsabelis, J. F. J. Engbersen and D. N. Reinhoudt, *J. Am. Chem. Soc.*, 1997, **119**, 2948.
- 28 P. Molenveld, J. F. J. Engbersen and D. N. Reinhoudt, *Eur. J. Org. Chem.*, 1999, 3269.
- 29 O. Iranzo, A. Y. Kovalevsky, J. R. Morrow and J. P. Richard, *J. Am. Chem. Soc.*, 2003, **125**, 1988.
- 30 K. P. McCue and J. R. Morrow, *Inorg. Chem.*, 1999, **38**, 6136.
- 31 T. Gajda, R. Kramer and A. Jancso, *Eur. J. Inorg. Chem.*, 2000, 1635.
- 32 M. Yashiro, A. Ishikubo and M. Komiyama, *J. Chem. Soc., Chem. Commun.*, 1995, 1793.
- 33 P. Rossi, F. Felluga, P. Tecilla, F. Formaggio, M. Crisma, C. Toniolo and P. Scrimin, *J. Am. Chem. Soc.*, 1999, **121**, 6948.
- 34 P. Rossi, F. Felluga, P. Tecilla, F. Formaggio, M. Crisma, C. Toniolo and P. Scrimin, *Biopolymers*, 2000, **55**, 496.
- 35 C. Sissi, P. Rossi, F. Felluga, F. Formaggio, M. Palumbo, P. Tecilla, C. Toniolo and P. Scrimin, *J. Am. Chem. Soc.*, 2001, **123**, 3169.
- 36 A. Scarso, U. Scheffer, M. Gobel, Q. B. Broxterman, B. Kaptein, F. Formaggio, C. Toniolo and P. Scrimin, *Proc. Natl. Acad. Sci. USA*, 2002, **99**, 5144.
- 37 N. V. Kaminskaia, C. He and S. J. Lippard, *Inorg. Chem.*, 2000, **39**, 3365.
- 38 C. He and S. J. Lippard, *J. Am. Chem. Soc.*, 2000, **122**, 184.
- 39 A. M. Barrios and S. J. Lippard, *Inorg. Chem.*, 2001, **40**, 1060.
- 40 B. Bauer-Siebenlist, F. Meyer, E. Farkas, D. Vidovic, J. A. Cuesta-Seijo, R. Herbst-Irmer and H. Pritzkow, *Inorg. Chem.*, 2004, **43**, 4189.
- 41 F. Meyer and P. Rutsch, *Chem. Commun.*, 1998, 1037.
- 42 C. Bazzicalupi, A. Bencini, A. Bianchi, V. Fusi, L. Mazzanti, P. Paoletti and B. Valtancoli, *Inorg. Chem.*, 1995, **34**, 3003.
- 43 C. Bazzicalupi, A. Bencini, A. Bianchi, V. Fusi, P. Paoletti and B. Valtancoli, *J. Chem. Soc., Chem. Commun.*, 1994, 881.
- 44 C. Bazzicalupi, A. Bencini, A. Bianchi, V. Fusi, L. Corana, V. Fusi, C. Giorgi, P. Paoli, P. Paoletti, B. Valtancoli and C. Zanchini, *Inorg. Chem.*, 1996, **35**, 5540.
- 45 C. Bazzicalupi, A. Bencini, A. Bianchi, V. Fusi, P. Paoletti and B. Valtancoli, *J. Chem. Soc., Chem. Commun.*, 1995, 1555.
- 46 C. Bazzicalupi, A. Bencini, A. Bianchi, V. Fusi, P. Paoletti, G. Piccardi and B. Valtancoli, *Inorg. Chem.*, 1995, **34**, 5622.
- 47 C. Bazzicalupi, A. Bencini, A. Bianchi, V. Fusi, C. Giorgi, P. Paoletti, B. Valtancoli and D. Zanchi, *Inorg. Chem.*, 1997, **36**, 2784.
- 48 A. Bencini, E. Berni, A. Bianchi, C. Giorgi and B. Valtancoli, *Supramol. Chem.*, 2001, **13**, 489.
- 49 A. Bencini, E. Berni, A. Bianchi, V. Fedi, C. Giorgi, P. Paoletti and B. Valtancoli, *Inorg. Chem.*, 1999, **38**, 6323.
- 50 C. Bazzicalupi, A. Bencini, E. Berni, A. Bianchi, V. Fedi, V. Fusi, C. Giorgi, P. Paoletti and B. Valtancoli, *Inorg. Chem.*, 1999, **38**, 4115.
- 51 M. Yashiro, A. Ishikubo and M. Komiyama, *Chem. Commun.*, 1997, 83.
- 52 C. Bazzicalupi, A. Bencini, E. Berni, C. Giorgi, S. Maoggi and B. Valtancoli, *Dalton Trans.*, 2003, 3574.
- 53 S. R. Korupolu, N. Mangayarkarasi, P. S. Zacharias, J. Mizuthani and H. Nishihara, *Inorg. Chem.*, 2002, **41**, 4099.
- 54 M. B. Dinger and M. J. Scott, *Eur. J. Org. Chem.*, 2000, 2467.
- 55 M. J. Plater, M. R. S. Foreman, T. Gelbrich and M. B. Hursthouse, *J. Chem. Soc., Dalton Trans.*, 2000, 1995.
- 56 S. Uhlenbrock, R. Wegner and B. Krebs, *J. Chem. Soc., Dalton Trans.*, 1996, 3731.

- 57 A. Looney, R. Han, I. B. Gorrell, M. Cornebise, K. Yoon, G. Parkin and A. L. Rheingold, *Organometallics*, 1995, **14**, 274.
- 58 J. C. M. Rivas, E. Salvagni, R. T. M. de Rosales and S. Parsons, *Dalton Trans.*, 2003, 3339.
- 59 E. Kinoshita, M. Takahashi, H. Takeda, M. Shiro and T. Koike, *Dalton Trans.*, 2004, 1189.
- 60 H. B. Collier, *Clin. Chem.*, 1979, **25**, 495.
- 61 J. E. Huheey, in *Inorganic Chemistry*, Harper, Cambridge, 1983, 3rd edn, p. 150.
- 62 C. Bleiholder, H. Borzel, P. Comba, R. Ferrari, M. Heydt, M. Kerscher, S. Kuwata, G. Laurency, G. A. Lawrance, A. Lienke, B. Martin, M. Merz, B. Nuber and H. Pritzkow, *Inorg. Chem.*, 2005, **44**, 8145.
- 63 A. E. Martell and R. J. Motekaitis, *Determination and Use of Stability Constants*, VCH, New York, 1992, 2nd edn.
- 64 A. E. Martell and R. M. Smith, *Critical Stability Constants*, Plenum Press, New York, 1982.
- 65 S. H. Gellman, R. Petter and R. Breslow, *J. Am. Chem. Soc.*, 1986, **108**, 2388.
- 66 P. Molenveld, J. F. J. Engbersen and D. N. Reinhoudt, *Angew. Chem., Int. Ed.*, 1999, **38**, 3189.
- 67 W. N. Lipscomb and N. Strater, *Chem. Rev.*, 1996, **96**, 2375.
- 68 B. Bennett and R. C. Holz, *J. Am. Chem. Soc.*, 1997, **119**, 1923.
- 69 X. D. Wang, R. Y. N. Ho, A. K. Whiting and L. Que, *J. Am. Chem. Soc.*, 1999, **121**, 9235.
- 70 T. Gajda, A. Jancso, S. Mikkola, H. Lonnberg and H. Sirges, *J. Chem. Soc., Dalton Trans.*, 2002, 1757.
- 71 C. Bazzicalupi, A. Bencini, E. Berni, A. Bianchi, P. Fornasari, C. Giorgi and B. Valtancoli, *Inorg. Chem.*, 2004, **43**, 6255.
- 72 P. Gettins and J. E. Coleman, *J. Biol. Chem.*, 1984, **259**, 4991.
- 73 L. Ma, T. T. Tibbitts and E. R. Kantrowitz, *Protein Sci.*, 1995, **4**, 1498.
- 74 F. Hollfelder and D. Herschlag, *Biochemistry*, 1995, **34**, 12255.
- 75 J. E. Murphy, T. T. Tibbitts and E. R. Kantrowitz, *J. Mol. Biol.*, 1995, **253**, 604.
- 76 S. Hansen, E. Hough, L. A. Svensson, Y. L. Wong and S. F. Martin, *J. Mol. Biol.*, 1993, **234**, 179.
- 77 S. F. Martin, Y. L. Wong and A. S. Wagman, *J. Org. Chem.*, 1994, **59**, 4821.
- 78 L. Bonfa, M. Gatos, F. Mancin, P. Tecilla and U. Toneliato, *Inorg. Chem.*, 2003, **42**, 3943.
- 79 D. M. Brown and D. A. Usher, *J. Chem. Soc.*, 1965, 6558.
- 80 E. Carceller, M. Merlos, M. Giral, C. Almansa, J. Bartroli, J. Garcia-rafanell and J. Forn, *J. Med. Chem.*, 1993, **36**, 2984.
- 81 M. B. Dinger and M. J. Scott, *Inorg. Chem.*, 2001, **40**, 856.
- 82 R. H. Blessing, *Acta Crystallogr., Sect. A*, 1995, **A51**, 33.
- 83 J. Bassett, R. C. Denney, G. H. Jeffery and J. Mendham, in *Titrimetric Analysis*, John Wiley & Sons, New York, 1978.
- 84 C. F. Bernasconi and W. T. Sun, *J. Am. Chem. Soc.*, 1993, **115**, 12526.
- 85 G. Gran, *Analyst*, 1952, **77**, 661.
- 86 F. J. Rossotti and H. Rossotti, *J. Chem. Educ.*, 1965, **42**, 375.